Membrane Type 1 Matrix Metalloproteinase-associated Degradation of Tissue Inhibitor of Metalloproteinase 2 in Human Tumor Cell Lines*

Erik Maquoi‡, Francis Frankenne‡, Eugenia Baramova‡, Carine Munaut‡, Nor Eddine Sounni‡, Albert Remacle‡, Agnès Noël‡§, Gillian Murphy¶, and Jean-Michel Foidart‡

From the ‡Laboratory of Tumor and Development Biology, University of Liège, Tour de Pathologie (B23), Sart Tilman, B-4000 Liège, Belgium and the ¶School of Biological Sciences, University of East Anglia, Norwich NR4 7TJ, United Kingdom

Abstract

Tissue inhibitor of metalloproteinase 2 (TIMP-2) is required for the membrane type 1 matrix metalloproteinase (MT1-MMP)-dependent activation of pro-MMP-2 on the cell surface. MT1-MMP-bound TIMP-2 has been shown to function as a receptor for secreted pro-MMP-2, resulting in the formation of a trimolecular complex. In the presence of uncomplexed active MT1-MMP, the prodomain of cell surface-associated MMP-2 is cleaved, and activated MMP-2 is released. However, the behavior of MT1-MMP-bound TIMP-2 during MMP-2 activation is currently unknown. In this study, ^{125}I-labeled recombinant TIMP-2 (^{125}I-rTIMP-2) was used to investigate the fate of TIMP-2 during pro-MMP-2 activation by HT1080 and transfected A2058 cells. HT1080 and A2058 cells transfected with MT1-MMP cDNA (but not vector-transfected A2058 cells) were able to bind ^{125}I-rTIMP-2, to activate pro-MMP-2, and to process MT1-MMP into an inactive 43-kDa form. Under these conditions, ^{125}I-rTIMP-2 bound to the cell surface was rapidly internalized and degraded in intracellular organelles through a bafilomycin A_1-sensitive mechanism, and ^{125}I-bearing low molecular mass fragment(s) were released in the culture medium. These different processes were inhibited by hydroxamic acid-based synthetic MMP inhibitors and rTIMP-2, but not by rTIMP-1 or cysteine, serine, or aspartic proteinase inhibitors. These results support the concept that the MT1-MMP-dependent internalization and degradation of TIMP-2 by some tumor cells might be involved in the regulation of pericellular proteolysis.

Abbreviation : MMPs, matrix metalloproteinases; MT1-MMP, membrane type 1 MMP; TIMP, tissue inhibitor of metalloproteinase; rTIMP, recombinant TIMP; TPA, 12-*O*-tetradecanoylphor-bol-13-acetate; ConA, concanavalin A; DMEM, Dulbecco's modified Eagle's medium; BSA, bovine serum albumin; ELISA, enzyme-linked immunosorbent assay; PBS, phosphate-buffered saline; PAGE, poly-acrylamide gel electrophoresis; pAbs, polyclonal antibodies.

Matrix metalloproteinases (MMPs), also known as matrixins, form a family of at least 19 structurally related neutral zinc endopeptidases. These MMPs are collectively able to degrade a wide variety of substrates, including extracellular matrix as well as non-extracellular matrix proteins (1). Consequently, MMPs are thought to be involved in a large number of both normal and pathological processes, including embryogenesis, wound healing, inflammation, and arthritis (2). Moreover, the association of MMPs with cancer cell invasion and metastasis has suggested that these proteinases represent an attractive target for the development of novel antitumoral therapies (3). Most members of the MMP family are produced as proenzymes consisting of an amino-terminal propeptide, a catalytic domain, and a hemopexin-like domain at the carboxyl terminus (2). The synthesis of most MMPs is specifically regulated at the level of gene expression (4). However, the catalytic activity of these proteinases is further controlled at additional levels, including activation of the proenzyme (by propeptide removal) and inhibition of the active enzyme by specific endogenous tissue inhibitors of MMPs, the TIMPs (5). Unlike most MMPs, MMP-2 (also known as gelatinase A) is constitutively secreted by many types of cells (6), and its activation involves a cell surface-anchored MMP possessing a hydrophobic C-terminal transmembrane domain. This enzyme was recently identified as membrane type 1 MMP (MT1-MMP or MMP-14) (7-12).

TIMP-2, a 21-kDa non-glycosylated MMP inhibitor that preferentially complexes with pro-MMP-2, has been shown to play a pivotal role in this activation process. Indeed, the active form of MT1-MMP, which is generated through a furin-dependent mechanism (13, 14), first binds TIMP-2 through its catalytic domain, thus docking soluble TIMP-2 to the cell surface. This bimolecular complex subsequently functions as a receptor for the secreted 66-kDa pro-MMP-2 through the interaction between the C-terminal domain of the enzyme and the C-terminal domain of TIMP-2 (15-19). In the presence of an adjacent free active MT1-MMP, the propeptide of MMP-2 is first cleaved between Asn[37] and Leu[38], generating an activated 62-kDa intermediate form. When present at a sufficiently high concentration on the cell surface, this intermediate form is further processed to fully activated 59-kDa MMP-2 by an intermolecular autolytic cleavage (7, 10, 15). Alternatively, this second cleavage can be achieved through the action of plasmin (20). When present in excess relative to active MT1-MMP, TIMP-2 completely blocks the first step of this activation process (7, 9, 10, 13, 18, 21, 22), thus emphasizing the key role of TIMP-2 in pro-MMP-2 processing: at low concentrations, it promotes the binding of pro-MMP-2 to MT1-MMP, whereas at higher concentrations, it prevents the activation process. Beyond its role in pro-MMP-2 activation, TIMP-2 is also involved in other biological activities, including cell adhesion (23), proliferation (24), and apoptosis (25), as well as stabilization of some MMPs (26). However, the most notable function of TIMP-2 is its capacity to form tight 1:1 stoichiometric complexes with active MMPs, resulting in the inhibition of the catalytic activity of these proteinases. In this context, an imbalance between the concentrations of active MMPs over TIMP-2, resulting in an increased proteolytic activity, has been implicated in tumor invasion and metastasis as well as angiogenesis (27). Conversely, exogenously added TIMP-2 has been shown to suppress growth, invasion, metastasis, and neovascularization in several tumor models (28-32). In accordance with these experimental observations, high MMP-2/TIMP-2 ratios have been associated with poor clinical outcomes in different tumor types (33-35).

We have demonstrated that pro-MMP-2 activation by HT1080 cells, a human fibrosarcoma cell line, was stimulated when these cells were either treated with 12-*O*-tetradecanoyl-phorbol-13-acetate (TPA) or concanavalin A (ConA) or plated on a thin coat of type IV collagen.[22] Interestingly, we observed that these different treatments concomitantly reduced the concentration of secreted TIMP-2 without affecting the TIMP-2 mRNA level, thus suggesting the potential occurrence of a post-transcriptional regulation of extracellular TIMP-2 concentration. In the current study, we have investigated the mechanism accounting for the reduced extracellular TIMP-2 level observed in TPA- and ConA-treated HT1080 cells. Our results demonstrate that TIMP-2 initially complexed to cell surface-anchored MT1-MMP is rapidly internalized and subsequently degraded, resulting in the depletion of extracellular TIMP-2.

EXPERIMENTAL PROCEDURES

Cell Culture

HT1080 human fibrosarcoma; MCF7, T47D, and BT549 human breast carcinoma; and A2058 human melanoma cells were maintained in Dulbecco's modified Eagle's medium (DMEM) supplemented with 10% (v/v) fetal calf serum, 100 IU/ml penicillin, 100 μg/ml streptomycin, 2 ml glutamine, and 10 mM Hepes buffer at 37 °C in a humid atmosphere (5% CO_2 and 95% air). All culture reagents were purchased from Life Technologies, Inc. (Merelbeke, Belgium).

Proteinase Inhibitors

The broad-spectrum hydroxamic acid-based synthetic MMP inhibitors GI129471 and BB-94 (36), AG3340 (37), and BB-2516 (38) were prepared as 10 mM stock solutions in dimethyl sulfoxide (Me$_2$SO) and used at final concentrations ranging from 0.01 to 10 μM in 0.1% Me$_2$SO. Human recombinant TIMP-2 (rTIMP-2) was obtained from transformed Chinese hamster ovary cell supernatants as described previously (20). Amiloride (5-500 μM), aprotinin (0.1-10 μM), E-64 (2.5-250 μM), soybean trypsin inhibitor (50-200 μg/ml), leupeptin (2-500 μg/ml), pepstatin A (5-20 μM), and phosphoramidon (31-250 μg/ml) were purchased from Sigma (Bornem, Belgium).

---

[2] E. Maquoi, F. Frankenne, E. Baramova, C. Munaut, N. E. Sounni, A. Remacle, A. Noël, G Murphy, and J.-M. Foidart, submitted for publication.

Transfection ofA2058 cells with MT1-MMP cDNA

A2058 cells were transfected, using LipofectAMINE (Life Technologies, Inc.), with either pc3MT1800S (human MT1-MMP cDNA cloned in the pcDNA3 expression plasmid) or pcDNA3 (control plasmid) vectors. Transfectants were isolated by selection with G418 (400 μg/ml). Three clones were selected: one transfected with the vector alone (C.IV.3) and two transfected with the MT1-MMP expression vector (S.I.3 and S.I.5). Expression of MT1-MMP was assessed by Northern and Western blotting as described below.

Preparation of Conditioned Media and Cell Extracts

Cells growing exponentially in T-75 flasks (Falcon Becton-Dickinson, Meylan, France) were harvested by trypsin/EDTA treatment, washed with 10% fetal calf serum-containing medium, and allowed to recover from trypsinization for at least 30 min at 37 °C. Cells were then washed twice with serum-free DMEM and diluted in the same medium supplemented with 0.1% bovine serum albumin (BSA; fraction V, Sigma) to a density of 6 x 10^5 cells/ml. This suspension (100 μl/well) was seeded in 96-well plates (Falcon). Cells were subsequently supplemented with 100 μl of serum-free DMEM (untreated control), ConA (final concentration of 30 μg/ml; Roche Molecular Biochemicals, Mannheim, Germany), or TPA (final concentration of 10 ng/ml; Sigma). In some experiments, proteinase inhibitors were also added. The resultant culture supernatants were collected after different incubation times and stored frozen at -20 °C. The resulting cell monolayers (60,000 cells) were washed once with 100 μl of serum-free DMEM and extracted with 50 μl of radioimmune precipitation assay buffer (50 mM Tris-HCl (pH 7.4), 150 ml NaCl, 1% Nonidet P-40, 1% Triton X-100, 1% sodium deoxycholate, 0.1% SDS, 5 mM iodoacetamide, and 2 mM phenylmethylsulfonyl fluoride) for 2 h at 4 °C. Alternatively (for enzyme-linked immunosorbent assay (ELISA)), cell monolayers were sonicated (10 s, 100 Hz) in 100 μl of phosphate-buffered saline (PBS) supplemented with 2 mM phenylmethylsulfonyl fluoride.

Iodination of rTIMP-2

rTIMP-2 was iodinated to a specific activity of 20-40 μCi/μg using the IODO-GEN technique (Pierce). Briefly, 0.8 mCi of ^{125}I$^-$ (Na^{125}I; Amersham Pharmacia Biotech, Gent, Belgium) was added to 10 μg of rTIMP-2 in 35 μl of 0.5 M sodium phosphate (pH 7.5). This solution was transferred into a 1.5-ml Eppendorf tube coated with 10 μg of IODO-GEN. After a 2-min incubation, the reaction was stopped by transferring the reaction mixture into 0.2 ml of 0.05 M sodium phosphate (pH 7.5). ^{125}I-rTIMP-2 was separated from free ^{125}I$^-$ and potentially aggregated forms by filtration through a 0.9 X 50-cm column (Econo column, Bio-Rad) of Sephacryl S200 resin (Amersham Pharmacia Biotech, Uppsala, Sweden). The integrity of iodinated rTIMP-2 was evaluated by SDS-15% PAGE, followed by autoradiography, which did not reveal any degradation after /3-mercaptoethanol (700 nM) reduction. ^{125}I-rTIMP-2 was also incubated with an excess of the recombinant catalytic domain of human MT3-MMP, and under these conditions, >90% of the inhibitor bound to the active site of the enzyme (data not shown). Finally, we confirmed that ^{125}I-rTIMP-2 was able to bind *in vivo* to the catalytic domain of plasma membrane-anchored MT1-MMP by demonstrating a specific binding of iodinated rTIMP-2 to transfected COS-1 cells overexpressing wild-type MT1-MMP, but not to cells overexpressing a catalytically inactive mutant form (Glu^{217} replaced by Ala) of MT1-MMP.[3]

Cell-surface Binding and Degradation of ^{125}I-rTIMP-2

Assays of ^{125}I-rTIMP-2 binding to cells plated in 96-well plates (see above) were performed in triplicate as follows. After adhesion, confluent cell monolayers were supplemented with ^{125}I-rTIMP-2 up to a final concentration of 0.6 nM for indicated culture periods. In some experiments, unlabeled rTIMP-1 (0.1 μM), unlabeled rTIMP-2 (0.1 μM), a synthetic MMP inhibitor (GI129471, 0.01-10 μM), or vehicle (0.1% Me$_2$SO) was added to the cells 10 min prior to the addition of ^{125}I-rTIMP-2. Nonspecific binding, which was evaluated by adding unlabeled rTIMP-2 in excess (500 nM), never exceeded 1% of the total added radioactivity. Cell monolayers were washed once with 100 μl of serum-free DMEM containing 0.1% BSA (DMEM/BSA) and extracted with 50 μl of radioimmune precipitation assay buffer supplemented with phenylmethylsulfonyl fluoride; the radioactivity associated with the total cell extracts was measured in a γ-counter. Specific binding was calculated by subtracting nonspecific radioactivity (see above) from cell extract-associated radioactivity measured in the absence of unlabeled rTIMP-2. Results are expressed as percentages of the total radioactivity

---

[3] A. Remacle, F. Frankenne, C. Munaut, E. Baramova, N. E. Sounni, S. Atkinson, A. Noël, G Murphy, and J.-M. Foidart, manuscript in preparation.

added per well. Culture supernatants were collected after different incubation periods, immediately mixed with an equal volume of sample buffer (with or without the reducing agent: 700 nM β-mercaptoethanol), and stored at 4 °C until electrophoresis. Samples were boiled for 5 min and subjected to SDS-15% PAGE. Once dry, gels were autoradiographed. The percentages of degraded radiolabeled rTIMP-2 were calculated based on densitometric analysis of autoradiographs. Specific ^{125}I-rTIMP-2 degradation was calculated by subtracting the percentage of spontaneous degradation (measured by incubating ^{125}I-rTIMP-2 in the absence of cells; this degradation ranged from 4 to 8% of the total radioactivity) from the percentage of degraded radiolabeled rTIMP-2 measured in the presence of cells.

Internalization Assay

Cells were prepared as described above and seeded in 24-well plates at a density of 10^6 cells/ml (500 μl/well) in serum-free DMEM/BSA. Assays of ^{125}I-rTIMP-2 internalization were performed in triplicate as follows. After adhesion, cell monolayers were incubated with ^{125}I-rTIMP-2 (0.6 nM) at 4 °C for 40 min. Free ligand was removed by two washings with serum-free DMEM/BSA at 4 °C. At time 0, prewarmed medium supplemented or not with ConA (30 μg/ml) was added (400 μl/well), and cell monolayers were then incubated at 37 °C for up to 180 min. At different times, culture supernatants were collected and precipitated with trichloroacetic acid at a final concentration of 12% (w/v), placed on ice for 60 min, and then centrifuged to separate acid-soluble (degraded) and acid-insoluble (intact) ^{125}I-rTIMP-2. The amount of cell surface-bound ^{125}I-rTIMP-2 was determined by subjecting the corresponding cell monolayers to acid washes (50 mM glycine HCl and 100 ml NaCl (pH 3)) for 2 x 2 min at 4 °C. The radioactivity remaining in the cells after the acid washes, defined as non-acid-extractable cell-associated radioactivity (internalized ^{125}I-rTIMP-2), was measured after dissolution of the cells in radioimmune precipitation assay buffer (200 μl/well). Radioactivities associated with cell lysates, acid washes, supernatants, and trichloroacetic acid-soluble materials were measured in a γ-counter. Results are expressed as percentages of ^{125}I-rTIMP-2 initially bound to the cell surface at time 0 (sum of radioactivities measured in cell lysates, acid washes, and supernatants).

Influence of Acidotropic Agents on TIMP-2 Synthesis and Degradation

Cell monolayers cultured in 96-well plates were treated for 24 h with either the weak base NH_4Cl (5-30 mM) or bafilomycin A_1 (0.1-100 nM dissolved in Me_2SO; Sigma). For control experiments, serum-free DMEM or Me_2SO (0.1%) was used. The influence of these drugs on TIMP-2 synthesis and degradation was evaluated by ELISA (see below) and trichloroacetic acid precipitation as described above under "Internalization Assay."

Gelatin Zymography

Analysis of gelatinolytic activities in supernatants and total cell extracts was performed by gelatin zymography. Test samples (10 μl) were mixed with equal volumes of sample buffer (62.5 mil Tris-HCl (pH 6.8), 2% SDS, 10% glycerol, and 0.1% bromphenol blue) and directly subjected to electrophoresis on 10% acrylamide gels containing 0.1% gelatin. Gels were run at 10 mA, washed with 2% Triton X-100 for 1 h, and incubated in activation buffer (50 mil Tris-HCl (pH 7.4), 200 mil NaCl, 5 mil $CaCl_2$, and 0.02% NaN_3) for 16 h at 37 °C. After staining with Coomassie Brilliant Blue R-250, the gelatinolytic activities were detected as clear bands against a blue background.

Western Blot Analysis of MT1-MMP

Samples of total cell extracts were analyzed using monoclonal antibody 2D7 directed against the hemopexin-like domain of MT1-MMP (kindly provided by P. Basset, Institut de Génétique et de Biologie Moléculaire et Cellulaire, Illkirch, France) as described previously (14), except that the proteins were transferred onto Immobilon-P membranes (Millipore Corp., Bedford, MA) using a Mini-Trans-Blot electrophoretic transfer cell device (Bio-Rad).

Isolation of RNA and Northern Blot Analysis

Total RNA was extracted from the cell monolayers by RNAzol B treatment (Biogenesis, Bournemouth, United Kingdom). An aliquot of RNA (15 μg) was electrophoresed on agarose gels containing 10% formaldehyde and transferred onto a nylon membrane (Hybond-N, Amersham Pharmacia Biotech). The membrane was hybridized with MMP-2, MT1-MMP, and TIMP-2 cDNA probes labeled with ^{32}P using random priming synthesis (Roche Molecular Biochemicals). The membrane was rehybridized to a human 28 S rRNA oligonucleotide probe (CLONTECH, Palo Alto, CA), used as an internal control. The amounts of the different transcripts were

quantified by densitometric analysis of autoradiographs of the Northern blots using a GS-700 imaging densitometer (Bio-Rad) equipped with Molecular Analyst software. All results were corrected for RNA loading as a function of the densitometric data obtained for the 28 S rRNA signals.

TIMP-1 and TIMP-2 Quantification by ELISA

TIMP-1 and TIMP-2 concentrations in supernatants and total cell extracts were determined using sandwich ELISAs. TIMP-1 was measured by using a commercial kit (Amersham Pharmacia Biotech, Roosendaal, The Netherlands) according to the manufacturer's instructions. rTIMP-2 (see above) was used to raise polyclonal antibodies (pAbs) in rabbits and in embryonated chicken eggs (SMI pAbs). The specific anti-rTIMP-2 IgGs from chicken were purified by ammonium sulfate precipitation (39). Rabbit pAbs were purified by affinity chromatography. Rabbit pAbs (diluted 1:750) were adsorbed onto Maxisorp 96-well plates (Nunc, Roskilde, Denmark) by overnight incubation at 4 °C. Wells were subsequently saturated overnight at 4 °C with 100 μl of PBS supplemented with 3% BSA and 0.05% Tween 20. Supernatants or total cell extract samples (50 μl) were added to each well and incubated overnight at 4 °C. After three washes with 200 μl of PBS and 0.05% Tween 20, 50 μl of the SM1 pAbs (diluted 1:200) were added for 1 h at 37 °C. The plate was again washed three times with 200 μl of PBS and 0.05% Tween 20, and 50 μl of peroxidase-conjugated rabbit anti-chicken IgG (diluted 1:10,000; Or-ganon Teknica, Turnhout, Belgium) were added for 1 h at 37 °C. After extensive washing with water, ABTS (750 mg/liter; Roche Molecular Biochemicals) and 0.004% H_2O_2 substrates in ABTS buffer (pH 5.6) were added for 1 h at 37 °C. Absorbances were measured at 405 nm using an automated microtiter plate reader (Multiscan MS, Lab-systems, Zellik, Belgium). The sensitivity of these ELISAs for TIMP-1 and TIMP-2 were 1.25 and 0.3 ng/ml, respectively, and the concentration *versus* absorbance curve was linear in the 3.13-50 and 0.6-20 ng/ml ranges, respectively. Each sample was run in duplicate. Results were finally expressed in nanograms/well.

Gel Filtration of Conditioned Media

Supernatant samples (1-2 ml) were loaded onto a 1 x 60-cm column of Superdex 75 resin (Amersham Pharmacia Biotech) equilibrated with PBS (pH 7.4) and 5 mil KI. A P60 pump (Amersham Pharmacia Biotech) eluted 2-ml fractions/min, which were subsequently counted in a γ-counter.

Reverse-phase Separation

To discriminate between the radioactivity peaks associated with free ^{125}I and peptide-bound ^{125}I, 1-ml aliquots from the gel-filtration low molecular mass peaks were loaded onto 1-ml Oasis columns (Waters Associates, Milford, MA) equilibrated with water. After a 2-ml wash with 5% ethanol, the bound material was eluted with 0.5 ml of 100% ethanol. The unbound fraction corresponds to the mixture of flow-through and wash eluates.

RESULTS

HT1080 Cells Bind and Degrade ^{125}I-rTIMP-2

In a previous study, we found that treatment of HT 1080 cells with TPA or ConA stimulated the activation of pro-MMP-2 and induced a marked decrease in the TIMP-2 level in the culture medium.[2] Although the exact mechanism accounting for this lower TIMP-2 level is currently unknown, it could not be ascribed to a reduction of the TIMP-2 mRNA level. We therefore hypothesized that it might result from either the degradation or modification of the localization of the secreted TIMP-2.

To investigate these hypotheses, we analyzed the fate of ^{125}I-rTIMP-2 (0.6 nM) added to HT1080 cells treated for up to 48 h with either TPA or ConA. Both culture supernatants and cell monolayers were collected at different times and subjected to SDS-PAGE and γ-counting, respectively (Fig. 1). When ^{125}I-rTIMP-2 was incubated in the absence of cells, SDS-PAGE analysis revealed the presence of a single band with an apparent molecular mass of ~21 kDa (Fig. 1*A*), corresponding to the intact inhibitor. After reduction, this band migrated with a slightly higher apparent molecular mass, in agreement with the presence of six disulfide bonds, which maintain the tertiary structure of the molecule. When ^{125}I-rTIMP-2 was incubated in the presence of HT 1080 cells, the intensity of the 21-kDa band decreased concomitantly with the appearance of an additional band, migrating just above the dye migration front (Fig. 1*A*). The migration of this low molecular mass band was not altered by reduction. Under these electrophoresis conditions, free ^{125}I appeared as a much more diffuse band at the migration front (data not shown).

To better define the nature of this low molecular mass band, we subjected the soluble ^{125}I-rTIMP-2 material to gel filtration and reverse-phase separation (Fig. 2). After Superdex 75 gel filtration of the supernatants of HT1080 cells cultured for 48 h with ^{125}I-rTIMP-2, the bulk of the radioactivity was found mainly in an elution volume corresponding to low molecular mass molecules (Fig. 2A). To rule out the possibility that this low molecular mass peak might represent free ^{125}I released from the radiolabeled rTIMP-2, ^{125}I (2 or 5 x 10^5 cpm) was mixed with the supernatant of HT1080 cells cultured for 48 h with ^{125}I-rTIMP-2 just prior to the filtration run. The elution profile (Fig. 2B) shows that ^{125}I was eluted in a volume distinct from that of the ^{125}I-rTIMP-2 degradation product. In addition, reverse-phase analysis of aliquots of the free ^{125}I-labeled fraction and the ^{125}I-rTIMP-2 degradation product fraction indicated that only the latter was adsorbed onto the resin. These data demonstrate that incubation of ^{125}I-rTIMP-2 with HT1080 cells yielded ^{125}I-bearing fragment(s) of low molecular mass eluting over an abnormally large elution volume on gel filtration, which probably results from interactions with the resin.

FIG. 1: *Degradation and binding of TIMP-2 by HT1080 cells. 125I-rTIMP-2 was added to either medium alone (Medium) or HT1080 cells incubated alone (Untreated) or in the presence of TPA(10 ng/ml) or ConA (30 μg/ml). After 24 and 48 h, supernatants and cell extracts were collected and subjected to SDS-PAGE (A and B), ELISA (C), and γ-counting (D). A, supernatants collected after 24 h were subjected to SDS-15% PAGE (with (+) or without (-) reduction by β-mercaptoetha-nol (β-ME)), followed by autoradiography of the gel. B, the percentages of degraded ^{125}I-rTIMP-2 were calculated after scanning densitometry of the autoradiographs of supernatants collected after 24 (□) and 48 h (■). C, concentrations of secreted and cell-associated (insert) endogenous TIMP-2 were measured by ELISA in supernatants and cell extracts harvested after 24 h (□) and 48 h (■). D, ^{125}I-rTIMP-2 binding to HT1080 cells after 24 h (□) and 48 h (■) was quantified by measuring the cell extract-associated radioactivity. Specific binding was calculated as the difference between bound radioactivity measured in the absence and presence of excess (500 nM) unlabeled TIMP-2 (nonspecific binding).*
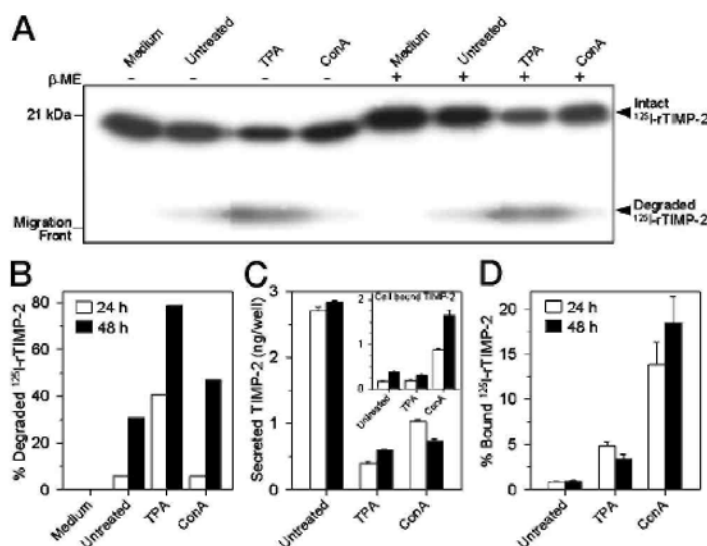

Scanning densitometry quantification of degraded ^{125}I-rTIMP-2 on autoradiographs revealed that, although TPA strongly increased the amount of degradation products in cells, exposure to ConA had only a minor effect (Fig. 1, A and B). The endogenous TIMP-2 concentration in the supernatant, as assessed by ELISA (Fig. 1C), was inversely related to the percentage of degraded ^{125}I-rTIMP-2 (Fig. 1B). This observation strongly suggests that the decreased concentration measured by ELISA after TPA treatment is a consequence of the TIMP-2 degradation. However, despite their limited ability to degrade ^{125}I-rTIMP-2, ConA-treated cells also released low levels of endogenous TIMP-2 into the supernatant, indicating that other mechanism(s) are probably involved in the modulation of the secreted TIMP-2 level. Because TIMP-2 has previously been shown to bind to the surface of several cell types (15, 19, 40), we measured the amount of TIMP-2 bound to ConA-treated HT1080 cells.

To investigate the binding of ^{125}I-rTIMP-2 to the surface, HT1080 cells were incubated for up to 48 h with ^{125}I-rTIMP-2. Total extracts were then evaluated by γ-counting (Fig. 1D). The results indicate that ~1% of the exogenously added ^{125}I-rTIMP-2 bound to untreated HT1080 cells. TPA treatment slightly increased the amount of cell-bound ^{125}I-rTIMP-2. In contrast, cells cultured with ConA had ~15-fold more bound ^{125}I-rTIMP-2 than untreated cells, thereby suggesting that the lower TIMP-2 level measured in supernatants of these cells essentially results from its increased binding to the cell surface. These data are in good agreement with the cell-

associated endogenous TIMP-2 levels determined by ELISA (Fig. 1C, *inset*). Analysis of these cell extracts by SDS-PAGE and autoradiography failed to detect the presence of cell-associated degraded ^{125}I-rTIMP-2 (data not shown).

FIG. 2: *Characterization of the ^{125}I-rTIMP-2 degradation product. HT1080 cells were incubated for 48 h in the presence of ^{125}I-rTIMP-2, and the supernatant was analyzed by gel filtration and reverse-phase separation. A, gel filtration analysis of the ^{125}I-rTIMP-2-containing supernatant revealed two distinct peaks of radioactivity encompassing fractions 40-50 (intact ^{125}I-rTIMP-2) and 74-87 (degraded ^{125}I-rTIMP-2). B, free ^{125}I (2 (●) or 5 (○) x 10^5 cpm) was mixed with the conditioned medium used in A and analyzed by gel filtration. Three peaks including fractions 40-50 (intact ^{125}I-rTIMP-2), 68-76 (free ^{125}I), and 76-87 (degraded ^{125}I-rTIMP-2) were detected. Aliquots of the two latter peaks (fractions 68-76 and 76-87) were subjected to reverse-phase analysis.*
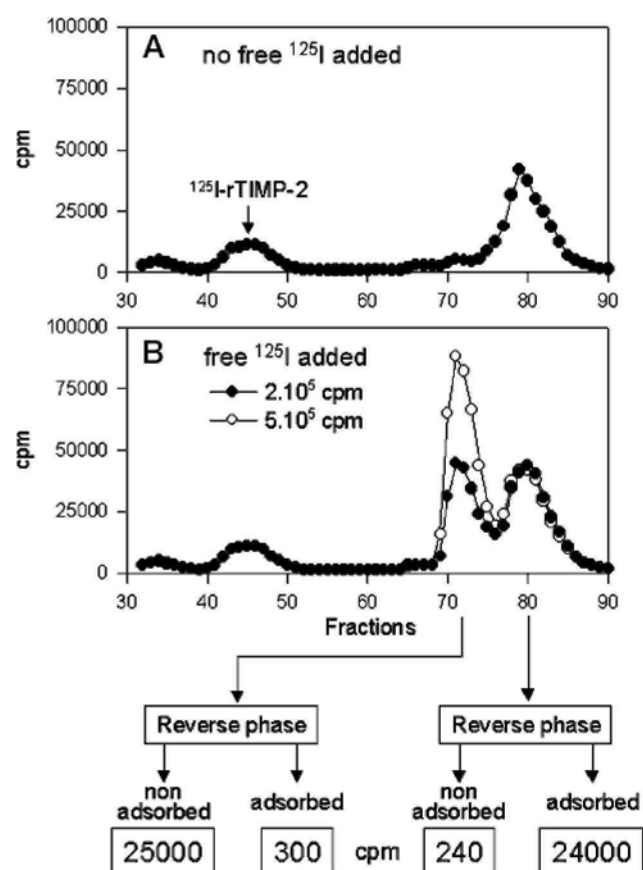
TIMP-2 Degradation Is Inhibited by Synthetic MMP Inhibitors

To further explore the mechanism of ^{125}I-rTIMP-2 degradation by HT1080 cells, we examined in greater detail the impact of TPA, the most efficient inducer of TIMP-2 degradation. We first attempted to identify the proteinase(s) involved in this degradation. For this purpose, HT1080 cells treated or not with TPA (10 ng/ml) were incubated with ^{125}I-rTIMP-2 in the presence of different proteinase inhibitors (Table I). Among these different inhibitors, only MMP inhibitors (GI129471, BB-94, BB-2516, and AG3340) prevented ^{125}I-rTIMP-2 degradation. These data are consistent with a role of metalloproteinases (but not cysteine, serine, or aspartic proteinases) in this degradation process.

As illustrated in Fig. 3 (A and *B*), GI129471 dose-dependently inhibited the degradation of both endogenous TIMP-2 (as assessed by ELISA) and ^{125}I-rTIMP-2 by HT1080 cells treated or not with TPA. Similar results were obtained with the three other synthetic MMP inhibitors used (data not shown). Complete inhibition of this degradation was obtained with the highest GI129471 concentrations (1 and 10 μM) (Fig. 3A, lanes 5 and 6). It is

worth noting that the progression of the endogenous TIMP-2 concentration as a function of the GI129471 dose was exactly opposite to that observed for the degradation of ^{125}I-rTIMP-2 (Fig. *3B*). This observation further supports the hypothesis that the appearance of ^{125}I-rTIMP-2 low molecular mass fragment(s) in the supernatant reflects the degradation of the endogenous protein, thereby accounting for the lower amounts detected by ELISA. To rule out the possibility that the different TIMP-2 concentrations induced by either TPA or GI129471 treatment could result from an altered mRNA level, TIMP-2 mRNA expression was analyzed by Northern blotting. Our data did not reveal any significant modification of the expression of this gene by these treatments (data not shown). It should be noted that the incubation of HT1080 cells in the presence of GI129471 did not alter the secretion of TIMP-1, another natural MMP inhibitor closely related to TIMP-2 (data not shown), suggesting that this degradation process is specific for TIMP-2.

TABLE I: *Effect of proteinase inhibitors on TIMP-2 degradation The proteinase inhibitors listed below were tested for their ability to inhibit the degradation of ^{125}I-rTIMP-2 as assessed by the quantification of low molecular mass degradation fragment(s) on SDS-PAGE.*

Compound	Cone, range	^{125}I-rTIMP-2 degradation % of control
Serine proteinase inhibitor		
Amiloride	5-50 μM	99.2 ± 2.4 (50 μM)[a]
Aprotinin	0.1-10 μM	98.8 ± 2.1 (10 μM)
Leupeptin	2-500 μg/ml	99.4 ± 4.3 (500 μg/ml)
Soybean trypsin inhibitor	50-200 μg/ml	100.3 ± 3.5 (200 μg/ml)
Aspartic acid proteinase inhibitor		
Pepstatin A	5-20 μM	96.8 ± 1.9 (4 μM)
Metalloproteinase inhibitor		
Phosphoramidon	31-250 μg/ml	102.1 ± 3.2 (250 μg/ml)
Matrix metalloproteinase inhibitor		
G1129471	0.01-10 μM	4.2 ± 3.6 (10 μM)
BB-94	0.01-10 μM	3.9 ± 2.7 (10 μM)
BB-2516	0.01-10 μM	5.7 ± 3.1(10 μM)
AG3340	0.01-10 μM	4.3 ± 2.2 (10 μM)
Cysteine proteinase inhibitor		
Leupeptin	2-500 μg/ml	98.7 ± 5.3 (500 μg/ml)
E-64	2.5-250 μM	99.5 ± 3.8 (250 μM)

[a] Inhibitor concentration resulting in the highest inhibition of ^{125}I-rTIMP-2 degradation.

GI129471 Prevents TIMP-2 Binding to HT1080 Cells

Quantification of ^{125}I-rTIMP-2 associated with HT1080 cells treated or not with TPA and incubated for 48 h in the presence of increasing concentrations of GI129471 revealed that, in the presence of this synthetic MMP inhibitor, the amount of cell-bound TIMP-2 was dose-dependently lower (Fig. 3C). This binding was completely abolished with GI129471 concentrations ranging from 1 to 10 µM. It should be noted that these inhibitor concentrations were also the most effective in preventing TIMP-2 degradation (Fig. 3B). Furthermore, a 48-h incubation at 37 °C of ^{125}I-rTIMP-2 with supernatants of HT1080 cells treated or not with TPA for 24 or 48 h failed to generate the TIMP-2 degradation fragment(s) observed in the presence of cells. These observations strongly suggest a cell surface-associated binding and degradation of TIMP-2.

TIMP-2 Degradation by HT1080 Cells Is Associated with Pro-MMP-2 Activation

In previous studies, the formation of bimolecular complexes of membrane-anchored active MT1-MMP and TIMP-2 molecules was shown to be a prerequisite for both the binding and activation of soluble pro-MMP-2 (10, 15, 16, 18, 41). Because GI129471 completely prevented the binding of ^{125}I-rTIMP-2 to HT1080 cells (Fig. 3C), we examined the possibility that this MMP inhibitor might also affect the MT1-MMP-dependent activation of pro-MMP-2. Processing of pro-MMP-2 by HT1080 cells was monitored by gelatin zymography of the supernatants of cells treated or not with TPA (10 ng/ml) and supplemented with increasing concentrations of

GI129471 (Fig. 4). In the absence of TPA, HT1080 cells slightly processed the 66-kDa pro-MMP-2 into a 62-kDa intermediate form, reflecting poor activation (Fig. 4A, *lane 1*). In contrast, TPA treatment strongly promoted pro-MMP-2 activation (Fig. 4A, *lane 5*). With or without TPA, GI129471 dose-dependently prevented MMP-2 activation, with inhibition of this processing being complete at 1 μM (Fig. 4A, *lanes 4 and 8*). Northern blotting revealed that, although TPA stimulated MT1-MMP mRNA expression, no difference in MT1-MMP expression was observed in the presence of the synthetic MMP inhibitor (data not shown). In contrast, Western blotting of total cell extracts revealed that GI129471 dramatically and qualitatively modified the MT1-MMP electrophoretic pattern (Fig. *AB*). Untreated HT1080 cells were characterized by a very low level of a 63-kDa pro-MT1-MMP and a 43-kDa band (Fig. *AB, lane 1*), recently identified as an MT1-MMP species lacking its active site (42). TPA treatment sharply increased the levels of the 63- and 43-kDa MT1-MMP species (Fig. *AB, lane 2*). When GI129471 was added to cells treated or not with TPA, the levels of the 43-kDa band were much weaker. In contrast, the 63-kDa species was more strongly expressed in conjunction with the appearance of a 60-kDa band corresponding to the active form of MT1-MMP (Fig. *AB, lane 3* and *4*). Altogether, these results indicate that, in HT1080 cells, TIMP-2 processing is closely associated with both the activation of pro-MMP-2 and the presence of the 43-kDa inactive MT1-MMP species.

Expression of MT1-MMP Is Necessary for TIMP-2 Degradation

We next evaluated in different tumor cell lines the correlation between the degradation of ^{125}I-rTIMP-2 and MT1-MMP expression. We also evaluated the effect of GI129471 treatment on the levels of endogenous TIMP-2 secreted in the medium (Table II). Our data indicate a close relationship between TIMP-2 degradation and the expression of a high level of MT1-MMP mRNA. In addition, MMP inhibition by GI129471 resulted in the accumulation of endogenous TIMP-2 in conditioned media only in those cell lines that express MT1-MMP.

To gain more insight into the potential involvement of MT1-MMP in the degradation of TIMP-2, A2058 human melanoma cells were stably transfected with either MT1-MMP cDNA (clones S.I.3 and S.I.5) or the control vector (clone C.IV.3). Northern blot characterization of these clones demonstrated that, in addition to the endogenous 4.5-kilobase MT1-MMP transcript that was weakly expressed by all three clones, S.I.3 and S.I.5 transfectants overexpressed a slightly shorter MT1-MMP mRNA species corresponding to the transgene (Fig. 5A). As a consequence of their low endogenous MT1-MMP mRNA content, C.IV.3 cells expressed barely detectable amounts of the corresponding protein, which was essentially present as the mature 60-kDa form (Fig. 6A, *lane 1*). On the other hand, high levels of MT1-MMP were detected in both S.I.3 (data not shown) and S.I.5 (Fig. 6C, *lane 1*) clones. In these two clones, the protein was mainly detected as the 43-kDa inactive species. The addition of increasing concentrations of GI129471 (Fig. 6, *A and C, lanes 2-4*) or rTIMP-2 (Fig. 6, *A and C, lanes 5*) led to lower expression of the 43-kDa MT1-MMP form, whereas the intensity of the 60-kDa band increased. rTIMP-1 had no effect on the MT1-MMP pattern (Fig. 6, *A and C, lanes 6*).

Analysis of the supernatants of the three clones by gelatin zymography revealed that, unlike C.IV.3, only the clones over-expressing MT1-MMP (S.I.3 and S.I.5) were able to generate both the intermediate (62-kDa) and fully mature (59-kDa) forms of pro-MMP-2 (Fig. 6, *B and D, lanes 1*). This activation process was dose-dependently prevented by GI129471 (Fig. *6D, lanes 2-4*) and rTIMP-2 (*lane 5*), but not by rTIMP-1 (*lane 6*).

ELISA quantification of secreted TIMP-2 indicated that, whereas C.IV.3 cells constitutively secreted high amounts of TIMP-2 (Fig. 7A, *bar group 1*), very low or undetectable levels were detected in the conditioned media of the S.I.3 (data not shown) and S.I.5 (Fig. *7B, bar group 1*) transfectants. This observation contrasts with the high TIMP-2 mRNA content observed by Northern blotting in both S.I.3 (data not shown) and S.I.5 (Fig. *5B*) transfectants, thereby suggesting the possible degradation of TIMP-2 by these two clones. Accordingly, when GI129471 was added, the TIMP-2 concentrations in the supernatants of these two clones were much higher (Fig. *IB, bar groups 2-4*) without affecting their TIMP-2 mRNA levels (Fig. *5B*). In contrast, GI129471 did not affect the level of TIMP-2 secreted by C.IV.3 cells (Fig. 7A, *bar groups 2-4*). To further confirm the degradation of TIMP-2 by clones overexpressing MT1-MMP (S.I.3 and S.I.5), exogenous ^{125}I-rTIMP-2 was added to the three clones. ^{125}I-rTIMP-2 bound strongly to both S.I.3 (data not shown) and S.I.5 (Fig. 8A) clones after 2 h, whereas C.IV.3 cells failed to bind significant amounts of ^{125}I-rTIMP-2 (*bar group 1*). This binding to S.I.5 cells was considerably reduced by the addition of GI129471 (Fig. *SA, bar groups 2-4*) and became undetectable when the cells were cultured with unlabeled rTIMP-2 (*bar group 5*). In contrast, rTIMP-1 did not alter this binding (Fig. *SA, bar group 6*). SDS-PAGE of the corresponding supernatants revealed that, although the C.IV.3 clone failed to degrade ^{125}I-rTIMP-2 (Fig. 8B, *lane 1*), S.I.3 (data not shown) and S.I.5 (Fig. 8C, *lane 1*) transfectants generated the typical TIMP-2 degradation band. This degradation process was completely abolished by the highest GI129471 concentration (Fig. 8C, *lane 4*) and rTIMP-2 (*lane 5*), but not by rTIMP-1 (*lane 6*).

FIG. 3: *GI129471 inhibits the degradation of TIMP-2 by HT1080 cells. HT1080 cells treated with TPA (10 ng/ml) or not (Ctl) were supplemented with increasing concentrations of GI129471 (0.01-10 µM) or vehicle alone (V, 0.1% Me₂SO) and incubated with ^{125}I-rTIMP-2. After 48 h, supernatants and cell extracts were collected and subjected to SDS-PAGE, sandwich ELISA, and γ-counting. A, cell extracts from HT1080 cells treated with TPA and supplemented with ^{125}I-rTIMP-2 were subjected to SDS-15% PAGE, followed by autoradiography of the gel. Lane 1 (Ctl), ^{125}I-rTIMP-2 incubated without cells; lane 2 (V), ^{125}I-rTIMP-2 incubated with HT1080 cells treated with 0.1% Me₂SO; lanes 3-6, ^{125}I-rTIMP-2 incubated with HT1080 cells treated with 0.01, 0.1, 1, and 10 µM GI129471, respectively. B, the percentages of degraded ^{125}I-rTIMP-2 in supernatants of HT1080 cells treated with TPA (●) or not (○) were calculated based on scanning densitometry of the corresponding autoradiographs (——), and the endogenous TIMP-2 concentration was measured by ELISA (- - -). C, binding of ^{125}I-rTIMP-2 to HT1080 cells treated with TPA (●) or not (○) was quantified by measuring the cell extract-associated radioactivity. Specific binding was calculated as the difference between bound radioactivity in the presence and absence of cells (nonspecific binding). Results are expressed as percentages of the specific binding measured in untreated cells. Error bars are S.D. values.*
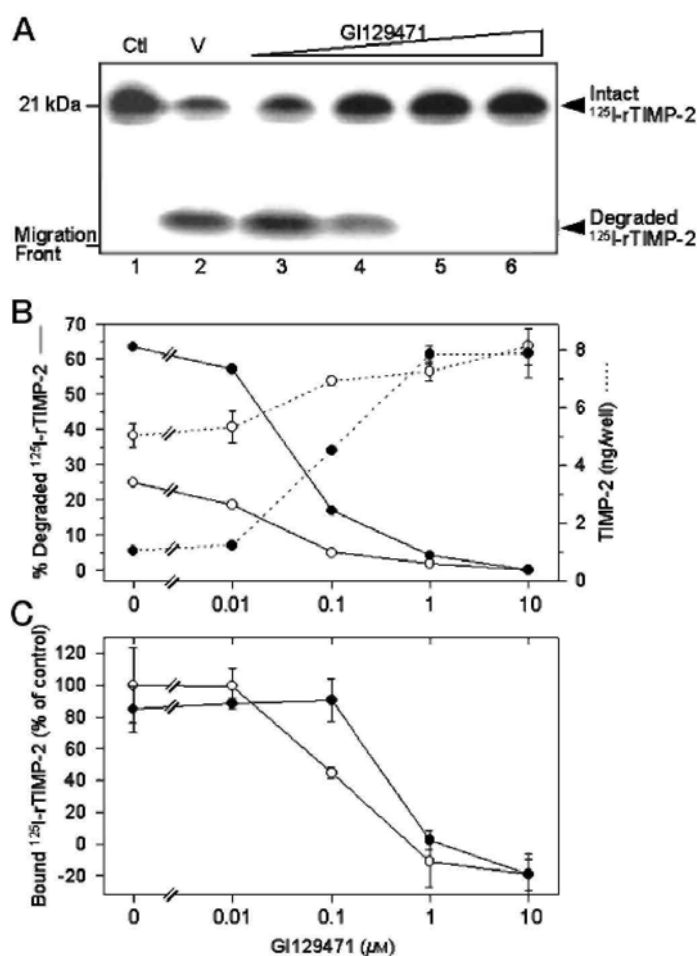

Membrane-bound ^{125}I-rTIMP-2 Is Rapidly Internalized and Degraded

To determine the fate of TIMP-2 after binding to the cell surface, S.I.5 cells were incubated with ^{125}I-rTIMP-2 (0.6 ᴍᴍ) at 4 °C for 40 min. After washing excess unbound ligand, the cells were transferred at 37 °C for various times, and the radioactivities recovered in the cell-associated form and in the supernatants were measured. Acid washing (see "Experimental Procedures") of the cell-associated radioactivity allowed for the discrimination between the cell surface-associated activity, accounting for the cell surface-bound ligand, and the intracellular activity, representing the internalized ^{125}I-rTIMP-2 (43). The level of ^{125}I-rTIMP-2 initially bound to the cell surface (cell-associated, acid-extracted radioactivity) decreased rapidly ($t_{1/2}$ = 20 min), and after 180 min at 37 °C, <5% of the initially bound ^{125}I-rTIMP-2 was found to be still surface-bound (Fig. 9A). The amount of internalized ligand (acid-resistant, cell-associated radioactivity) increased rapidly, reaching ~60% of the total radioactivity after 30 min, and decreased thereafter. Quantification of the radioactivity present in the supernatants showed that it increased rapidly during the first hour of incubation, reaching 85% of the total

radioactivity after 120 min. Precipitation of these supernatants by 12% trichloroacetic acid revealed that most of this radioactivity was trichloroacetic acid-soluble and represented thus degraded ^{125}I-rTIMP-2 (Fig. 9A). The time course indicates a precursor-product relationship between the internalized and degraded ^{125}I-rTIMP-2, suggesting that cell surface-bound ^{125}I-rTIMP-2 is internalized, degraded thereafter, and released in the medium in a degraded form.

FIG. 4: GI129471 inhibits the activation of pro-MMP-2 and reduces the processing of MT1-MMP by HT1080 cells. A, HT1080 cells cultured in the absence (lanes 1-4) or presence (lanes 5-8) of TPA (10 ng/ml) were supplemented with either increasing concentrations of GI129471 (0.01, 0.1, and 1 μM; lanes 2-4 and 6-8, respectively) or vehicle alone (V, 0.1% Me₂SO; lanes 1 and 5). After 48 h, supernatants were collected and subjected to gelatin zymography. B, HT1080 cells cultured in the absence (lanes 1 and 3) or presence (lanes 2 and 4) of TPA (10 ng/ml) were supplemented with GI129471 (1 μM; lanes 3 and 4) or vehicle alone (0.1% Me₂SO; lanes 1 and 2). Cell extracts were prepared after 48 h of incubation and subjected to Western blotting using monoclonal antibody 2D7 directed against the hemopexin-like domain of MT1-MMP.
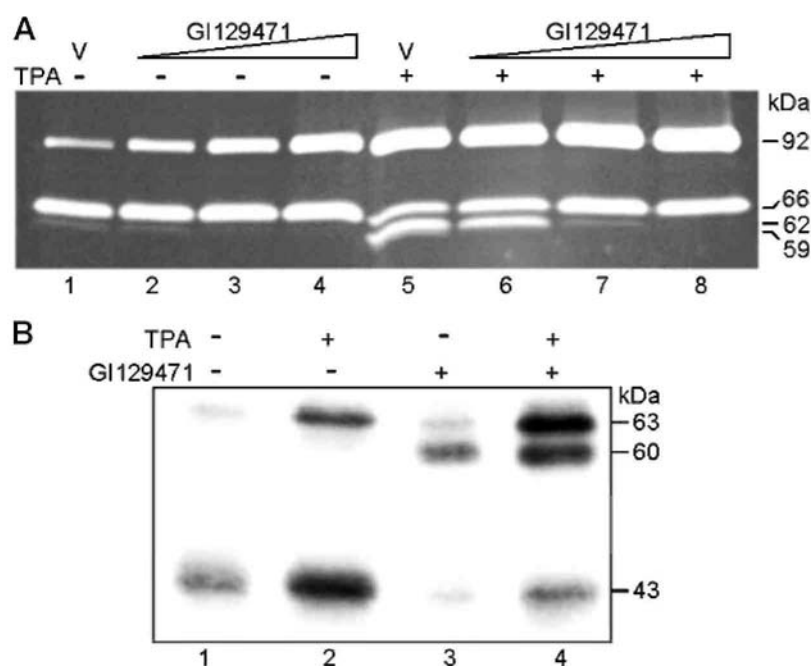
TABLE II: *Relationship between MT1-MMP expression and ^{125}I-rTIMP-2 degradation in the absence or presence of GI129471 (1 μM) in different human tumor cell lines*

Cell line	MT1-MMP mRNA[a]	^{125}I-rTIMP-2 degradation	
		0 μM GI129471	1 μM GI129471
		% of total radioactivity	
HT1080 (fibrosarcoma)	1.2 ± 0.1	25 ±6	3 ± 2
T47D (breast carcinoma)	0	0	0
MCF7 (breast carcinoma)	0	0	0
BT549 (breast carcinoma)	1.3 ± 0.2	23 ±9	10 ±3
A2058, clone C.IV.3 (melanoma)	0.4 ± 0.1	3 ± 1	0
MT1-MMP-transfected A2058			
Clone S.I.3	2.2 ± 0.3	71 ±8	11 ± 5
Clone S.I.5	1.8 ± 0.2	66 ±4	7 ± 2

[a] Levels of MT1-MMP transcripts were quantified by densitometric analysis of the Northern blots. Data were corrected for RNA loading by densitometric data obtained for the 28 S rRNA. Results are expressed as the ratio of the optical density of MT1-MMP to the optical density of 28 S rRNA (mean ± S.D.).

[b] Cells treated with GI129471 (1 μM) or vehicle alone (0.1% Me₂SO) were incubated with ^{125}I-rTIMP-2 for 48 h. Supernatants were collected and subjected to SDS-PAGE, and ^{125}I-rTIMP-2 degradation was quantified by scanning densitometry of the autoradiographs. Results are expressed as mean ± S.D.

To characterize further this internalization process, we performed a similar experiment as described above except that ConA (30 μg/ml) was added when the cells were transferred at 37 °C (time 0). Due to its ability to irreversibly cross-link membrane glycoproteins including MT1-MMP (44), ConA is thought to interfere with the translocation of membrane receptors to their sites of endocytosis (45, 46), thus reducing the internalization of their ligands. In the presence of ConA, internalized ^{125}I-rTIMP-2 did not peak after 30 min, but remained constant for up to 180 min ($t_{1/2}$ = 60 min), accounting for ~40% of the initially bound radioactivity (Fig. *9B*). As a consequence of this reduced internalization, the release of trichloroacetic acid-soluble ^{125}I-rTIMP-2 degradation fragments in the supernatants was reduced by >50% when compared with untreated cells (Fig. 9, compare *A* and *B*).

Since once internalized, ^{125}I-rTIMP-2 is released in the medium in a degraded form, it seemed likely that TIMP-2 enters intracellular acidic compartments such as endosomes and lysosomes, where it is subsequently degraded. We thus tested whether increasing the pH of these intracellular compartments with acidotropic agents can alter the processing of TIMP-2. For this purpose, S.I.5 cells were incubated with ^{125}I-rTIMP-2 (0.6 nM) in the presence of increasing concentrations of NH_4Cl or bafilomycin A_1, a highly specific inhibitor of the vacuolar ATPase (47). After a 24-h incubation period, supernatants were collected and precipitated with trichloroacetic acid. Bafilomycin A_1 dose-dependently promoted the accumulation of ^{125}I-rTIMP-2 associated with the cells (Fig. 10*B*) and dramatically reduced its release in the supernatant in a degraded form (Fig. 10*A*). Quantification of endogenous TIMP-2 production in bafilomycin A_1-treated cells (as measured by ELISA) demonstrated the increase in both secreted (Fig. 10*C*) and cell-associated (Fig. 10*D*) TIMP-2 in the presence of this drug. Similar results were obtained after treatment with 50 mM NH_4Cl (data not shown). Altogether, these results suggest that the degradation of internalized TIMP-2 relies on the acidification of intracellular organelles such as endosomes and/or lysosomes.

DISCUSSION

We previously observed that, in HT1080 cells, pro-MMP-2 activation induced by TPA or ConA was accompanied by a low concentration of TIMP-2 in the supernatant.[2] Based on their recent study, Shofuda *et al.* (48) suggested that the abilities of different human cancer cell lines to activate pro-MMP-2 is associated with both the expression of MT1-MMP and a non-transcriptionally regulated reduction of TIMP-2 secretion.

The results presented here demonstrate that different human tumor cell lines, including HT1080, BT549, and MT1-MMP-transfected A2058 cells, are able to degrade TIMP-2 into small peptide(s). The degradation by untreated HT1080 cells was relatively inefficient (only 30% of ^{125}I-rTIMP-2 was degraded after 48 h), but was markedly enhanced upon TPA treatment (>65% degraded ^{125}I-rTIMP-2). Although the activation of pro-MMP-2 in our cell culture models was induced artificially (TPA treatment of HT1080 cells and MT1-MMP cDNA transfection of A2058 cells), a similar relationship between MMP-2 activation and TIMP-2 degradation was observed when HT1080 cells were plated on a thin coat of type IV collagen,[2] thereby suggesting the physiological relevance of this process.

FIG. 5: *MT1-MMP and TIMP-2 mRNA expression in A2058 clones treated or not with GI129471. The three A2058 clones (C.IV.3, S.I.3, and S.I.5) were cultured for 24 h in the presence of GI129471 (1 µM; ■) or vehicle alone (0.1% Me₂SO; □). Left panels, total RNA was extracted and subjected to Northern blotting with MT1-MMP (A) and TIMP-2 (B) probes. The arrow indicates mRNA corresponding to transfected MT1-MMP cDNA Right panels, the different transcripts were quantified by densitometric analysis of the blots. All results were corrected for RNA loading by densitometric data obtained for the 28 S rRNA signals. kb, kilobase.*
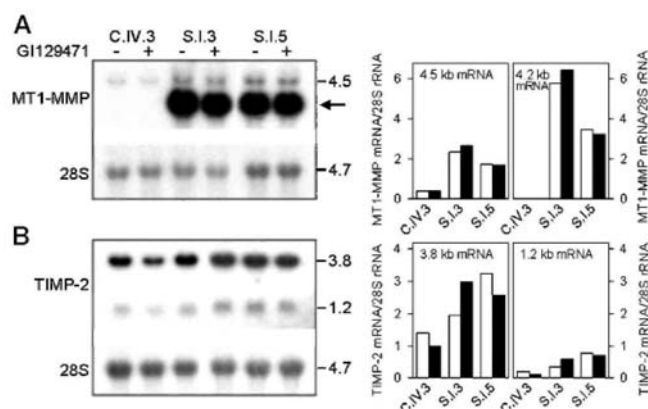
FIG. 6: *Expression of MT1-MMP and activation of pro-MMP-2 in A2058 clones. C.IV.3 (A and B) and S.I.5 (C and D) clones were treated with increasing concentrations of GI129471 (0.01, 0.1, and 1 μM; lanes 2-4, respectively), rTIMP-2 (0.1 μM; lane 5), rTIMP-1 (0.1 μM; lane 6), or vehicle alone (V, 0.1% Me$_2$SO; lane 1). After 48 h, supernatants were collected, and cell extracts were prepared. The latter were subjected to Western blotting using monoclonal antibody 2D7 directed against the hemopexin-like domain of MT1-MMP (A and C), and supernatants were subjected to gelatin zymography (B and D).*
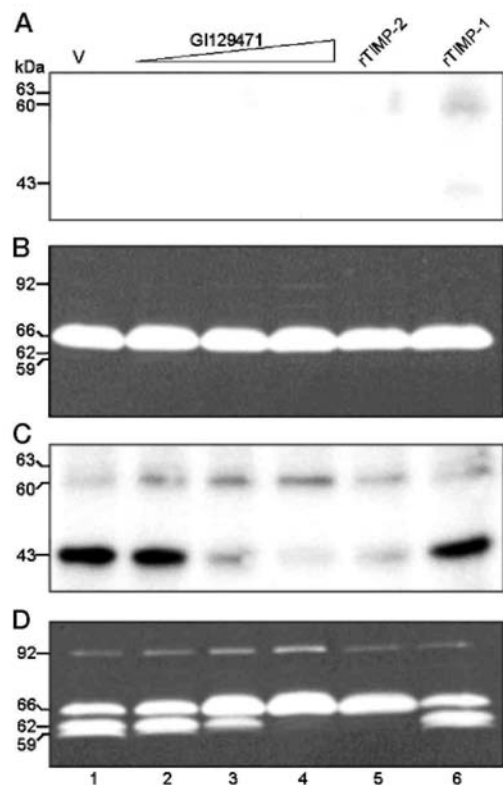
FIG. 7: *MMP inhibitor modulation of endogenous TIMP-2 secretion by A2058 clones. C.IV.3 (A) and S.I.5 (B) clones were exposed to increasing concentrations of GI129471 (0.01, 0.1, and 1 μM; bar groups 2-4, respectively) or 0.1% Me$_2$SO (vehicle (V); bar group 1). Supernatants were collected after 2 h (▨), 24 h (■), and 48 h (■), and TIMP-2 levels were assessed by sandwich ELISA.*
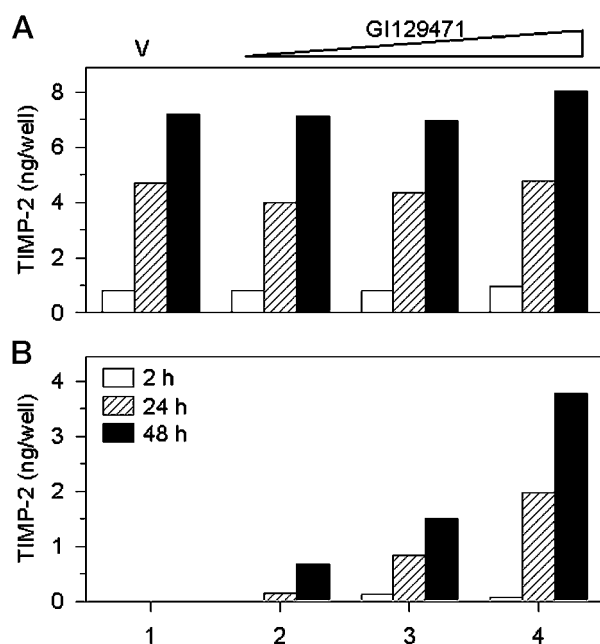
The observation that TIMP-2 degradation could not be reproduced by the incubation of ^{125}I-rTIMP-2 with HT1080 cell supernatants strongly suggests that this process requires the binding of TIMP-2 to the cell surface. However, the distinct abilities of cells to bind and to degrade TIMP-2 (as observed with ConA- *versus* TPA-treated HT1080 cells) indicate that TIMP-2 binding to the cell surface is not sufficient for degradation to occur.

To characterize the mechanism of TIMP-2 degradation, ^{125}I-rTIMP-2 was incubated with HT1080 cells in the presence of inhibitors of different proteinases, including MMPs and cysteine, serine, and aspartic acid proteinases. Among these inhibitors, only synthetic MMP inhibitors effectively prevented both basal and TPA-stimulated degradation of TIMP-2, thus suggesting the involvement of at least one active MMP in this degradation process. However, since these inhibitors also blocked the binding of ^{125}I-rTIMP-2 to the cell surface, their protective effect against TIMP-2 degradation could result from their ability to displace TIMP-2 from its cell-surface receptor rather than from their anti-proteolytic activity.

Because MMP inhibitors also prevented the TPA-induced activation of pro-MMP-2 by HT1080 cells, a process that was previously demonstrated to require the binding of TIMP-2 to active MT1-MMP on the cell surface (15, 16, 18), we hypothesized that MT1-MMP could play a role in both TIMP-2 binding and degradation. Western blot analysis of MT1-MMP expression in HT1080 cell extracts revealed that, in untreated cells, MT1-MMP was detected as a minor 63-kDa form, corresponding to the proenzyme, and a major species of 43 kDa. This latter species was previously identified as a cell surface-associated N-terminally truncated MT1-MMP lacking its active site (42, 49) and was detected in association with MMP-2 activation (17, 42, 49-51). In agreement with these data, TPA treatment of HT1080 cells, in addition to stimulating MMP-2 activation and TIMP-2 degradation, sharply increased the level of the 43-kDa form of MT1-MMP. Furthermore, we found that, in the presence of a synthetic MMP inhibitor, HT1080 cells contained much less 43-kDa MT1-MMP, concomitant with the accumulation of the active 60-kDa MT1-MMP species. Despite the presence of this active MT1-MMP, pro-MMP-2 activation was prevented by the synthetic MMP inhibitor.

FIG. 8: ^{125}I-rTIMP-2 binding to and degradation by A2058 clones. C.IV.3 and S.I.5 clones were exposed to increasing concentrations of GI129471 (0.01, 0.1, and 1 µM; bar groups I lanes 2-4, respectively), rTIMP-2 (0.1 µM; bar group/lane 5), rTIMP-1 (0.1 µM; bar group/lane 6), or 0.1% Me$_2$SO (vehicle (V); bar group/lane 1), and ^{125}I-rTIMP-2 was added. A, the radioactivity associated with C.IV.3 (□) and S.I.5 (■) cells was quantified by γ-counting after a 2-h incubation. Specific binding was calculated as the difference between bound radioactivity measured in the absence and presence of excess (500 nM) unlabeled TIMP-2 (nonspecific binding). B and C, supernatants from C.IV.3 and S.I.5 clones, respectively, were harvested after 24 h and subjected to SDS-15% PAGE, followed by autoradiography of the gel.
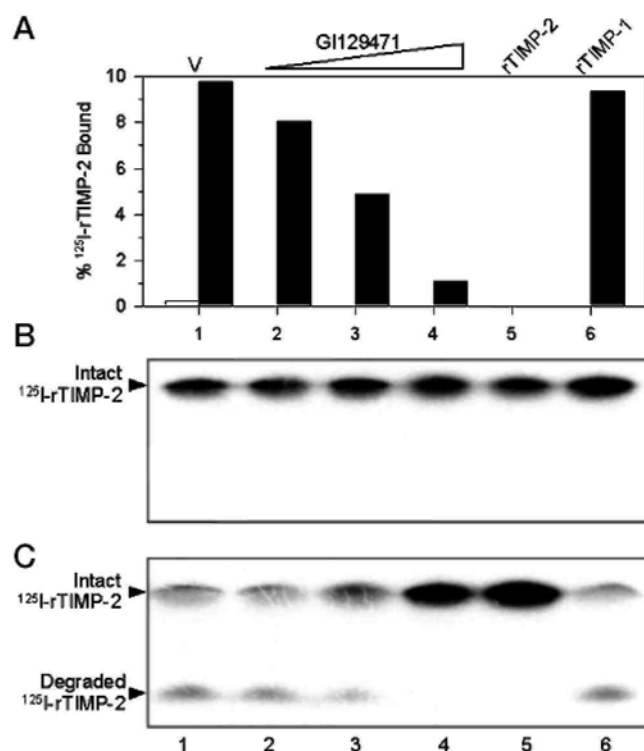
Our observations, in accordance with previously published data (42, 51), suggest that the 43-kDa MT1-MMP is a product of an MMP-dependent proteolysis of the 60-kDa species and is linked to MMP-2 maturation. Taken together, these data clearly imply that the degradation of TIMP-2 by TPA-treated HT1080 cells is closely associated with their capacity to bind TIMP-2, to activate pro-MMP-2, and to generate an inactive form of MT1-MMP, pointing to the potential involvement of MT1-MMP in these different processes.

To further investigate this possibility, we examined the ability of MT1-MMP-transfected A2058 cells to degrade TIMP-2.

Control A2058 cells (C.IV.3 clone) expressed very low levels of MT1-MMP and secreted high levels of TIMP-2. As a consequence of this imbalance between TIMP-2 and MT1-MMP levels, these cells failed to activate endogenously secreted pro-MMP-2, even after TPA or ConA treatment (data not shown), and were unable to bind and to degrade ^{125}I-rTIMP-2. Transfection of A2058 cells with an MT1-MMP vector (S.I.3 and S.I.5 clones) induced an overexpression of MT1-MMP and endowed the cells with the ability to bind ^{125}I-rTIMP-2 and to activate pro-MMP-2 at their surface. In contrast to control A2058 cells, the conditioned medium of MT1-MMP-overexpressing cells contained very low levels of intact endogenous TIMP-2, and ^{125}I-rTIMP-2 added to the cell cultures was readily degraded, identifying MT1-MMP as an element essential for TIMP-2 degradation to occur. Additional evidence for a role of MT1-MMP in this process came from the observation that, in MT1-MMP-transfected A2058 cells, MMP-2 activation and TIMP-2 binding and degradation were prevented by synthetic MMP inhibitors and rTIMP-2, but not by rTIMP-1. This specific inhibitory profile was previously reported to be characteristic of MT1-MMP(10,18,19,21,49,52).

In an attempt to further characterize the fate of cell-bound TIMP-2, we observed that ^{125}I-rTIMP-2 initially bound to the surface of MT1-MMP-transfected A2058 cells at 4 °C was rapidly internalized when the cells were chased at 37 °C. Internalized ^{125}I-rTIMP-2 was rapidly degraded in intracytoplasmic organelles and was finally released in the supernatant as low molecular mass degradation fragments. Indeed, most of the ^{125}I-rTIMP-2 initially bound to the cell surface was found in the supernatants in a degraded form after a 180-min incubation at 37 °C. When chasing was performed in the presence of ConA, ^{125}I-rTIMP-2 internalization and degradation were markedly reduced. This observation thus suggests that the cross-linking of membrane glycoproteins, including MT1-MMP, triggered by ConA potentially prevented MT1-MMP from moving to specialized regions of the plasma membrane such as coated pits where receptor-mediated endocytosis takes place (53). ConA was recently shown to promote the aggregation of MT1-MMP on dorsal cell surfaces, thus preventing its localization in membrane protrusions observed in contact with the extracellular matrix (44). Interestingly, this treatment, although increasing pro-MMP-2 activation, was shown to sharply decrease extracellular matrix degradation as well as invasiveness of melanoma cells overexpressing MT1-MMP, revealing that the precise localization of MT1-MMP on the plasma membrane may be essential for at least some of the functions of this MMP (44). Altogether, these different data might well account for our observation that ConA-treated HT1080 cells, despite their higher capacity to bind TIMP-2, did not efficiently degrade it.

In this study, we show that the treatment of MT1-MMP-transfected A2058 cells with bafilomycin A_1, a drug that specifically prevents the acidification of endosomes as well as lysosomes (47), leads to a nearly complete inhibition of the release of degraded ^{125}I-rTIMP-2 into the culture medium and to the accumulation of huge amounts of cell-associated intact TIMP-2. These observations demonstrate the requirement for an acidic endosomal/lysosomal pH for TIMP-2 degradation to occur. Although our results do not definitely identify the mechanism by which bafilomycin A_1 prevents TIMP-2 degradation, several data from the literature suggest that this drug does not affect the internalization of ligand-receptor complexes, but rather blocks either the routing of internalized molecules to the lysosomes (54) or the transport of lysosomal proteinases from the Golgi to the lysosomes (55).

In conclusion, our data suggest that the MT1-MMP-depend-ent degradation of TIMP-2 is a process that involves the internalization of MT1-MMP-bound TIMP-2, followed by an extensive cleavage process occurring in intracellular organelles such as endosomes or lysosomes through a pH-sensitive mechanism. The fate of MT1-MMP after internalization remains an open question. One possibility is that it may be delivered to the endosomes/lysosomes and degraded. Alternatively, intact or modified MT1-MMP might recycle back to the plasma membrane. We are currently investigating these hypotheses.

FIG. 9: ^{125}I-rTIMP-2 internalization and degradation by S.I.5 cells. S.I.5 cells were incubated with ^{125}I-rTIMP-2 (0.6 nM) for 40 min at 4 °C. After removing free ligand, prewarmed medium supplemented (B) or not (A) with ConA (30 µg/ml) was added at time 0, and cell monolayers were incubated at 37 °C for up to 180 min. At different times, culture supernatants were collected and measured in a γ-counter to quantify the total radioactivity released (○). Supernatants were subsequently precipitated with 12% trichloroacetic acid (TCA) to separate trichloroacetic acid-soluble (degraded; ●) from trichloroacetic acid-insoluble (intact) ^{125}I-rTIMP-2. Cell surface-bound ^{125}I-rTIMP-2 (acid-soluble radioactivity; ■) was quantified by subjecting the cells to acid washes (50 ml glycine HC1 and 100 mM NaCl (pH 3)). The radioactivity remaining in the cells after the acid washes was defined as internalized ^{125}I-rTIMP-2 (acid-resistant, cell-associated radioactivity; Δ). Radioactivities associated with cell lysates, acid washes, supernatants, and trichloroacetic acid-soluble materials were measured in a γ-counter. Results are expressed as percentages of ^{125}I-rTIMP-2 initially bound to the cell surface at time 0 (sum of radioactivities measured in cell lysates, acid washes, and supernatants).
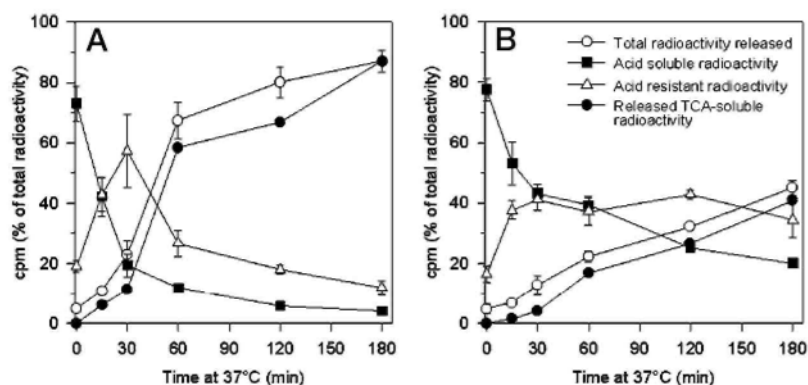
FIG. 10: Influence of bafilomycin A_1 on endogenous TIMP-2 and ^{125}I-rTIMP-2 degradation by S.I.5 cells. S.I.5 cells supplemented (A and B) or not (C and D) with ^{125}I-rTIMP-2 were treated with increasing concentrations of bafilomycin A_1 (0-100 nM). After 24 h, cell supernatants (A and C) were collected, and the corresponding cell monolayers (B and D) were extracted. Degraded ^{125}I-rTIMP-2 present in the supernatants (A) was quantified by trichloroacetic acid precipitation (see "Experimental Procedures"). The levels of cell-associated endogenous TIMP-2 (D) and radiolabeled rTIMP-2 (B) were evaluated by ELISA and γ-counting, respectively. TIMP-2 levels in the supernatants were measured by ELISA (C).
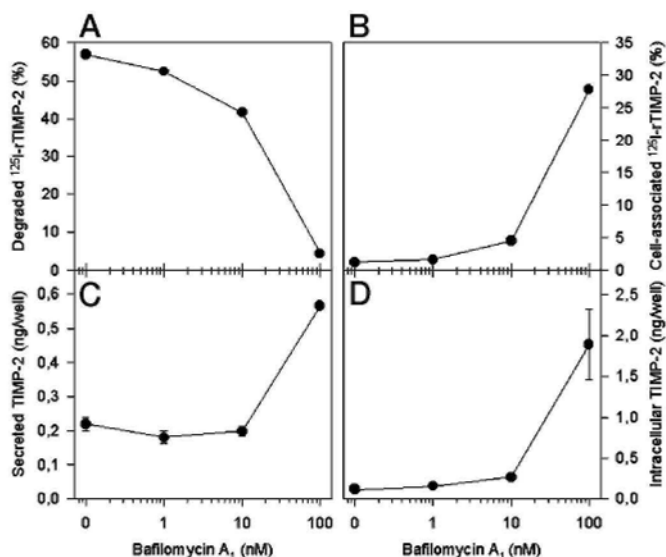
According to previous reports (16, 18), the activation of pro-MMP-2 at the cell surface is regulated by the balance between MT1-MMP complexed by TIMP-2 (which functions as a receptor for MMP-2) and TIMP-2-free MT1-MMP (which functions as an activator of MT1-MMP-bound MMP-2). When present at low concentrations, TIMP-2 binds to the catalytic site of some activated MT1-MMP molecules (19), generating receptors for pro-MMP-2, thereby promoting MMP-2 activation. At higher concentrations, TIMP-2 binds and inhibits any active MT1-MMP, thus completely preventing MMP-2 activation. Our observation that MT1-MMP-

bound TIMP-2 is internalized and subsequently degraded suggests that this degradation process could represent an upstream mechanism that regulates the concentration of cell surface-associated TIMP-2, thus indirectly controlling the binding and hence the activation of pro-MMP-2. Alternatively, it could be a downstream event that results from the processing of MT1-MMPTIMP-2-MMP-2 trimolecular complexes, as described previously for the urokinase plasminogen activator receptor-urokinase plasminogen activator-plasminogen activator inhibitor complexes (56).

It should be noted that the degradation of TIMP-2 illustrated here potentially represents an additional mechanism regulating the proteolytic activity of the cell. Indeed, because the net proteolytic activity is determined by the balance between the levels of active proteinases and their corresponding inhibitors (57), the ability of the cell to decrease extracellular TIMP-2 concentration (through its degradation) will alter this balance, leading to an increased degradative capacity. Finally, it is interesting to note that the higher concentration of secreted TIMP-2 observed in the presence of the synthetic MMP inhibitors might contribute to the anti-invasive and anti-metastatic properties of these compounds (58, 59).

ACKNOWLEDGMENTS

REFERENCES

1. Werb, Z. (1997) *Cell* 91, 439-442

2. Woessner, J. F. (1998) in *Matrix Metalloproteinases* (Parks, W. C, and Mecham, R. P., eds) pp. 1-14, Academic Press, Inc., San Diego, CA

3. Brown, P. D. (1999) *APMIS* 107, 174-180

4. Fini, M. E., Cook, J. R., Mohan, R., and Brinckerhoff, C. E. (1998) in *Matrix Metalloproteinases* (Parks, W. C, and Mecham, R. P., eds) pp. 299-356, Academic Press, Inc., San Diego, CA

5. Nagase, H. (1997) *Biol. Chem.* 378, 151-160

6. Yu, A. E., Hewitt, R. E., Kleiner, D. E., and Stetler-Stevenson, W. G. (1996) *Biochem. Cell Biol.* 74, 823-831

7. Strongin, A. Y., Mariner, B. L., Grant, G. A, and Goldberg, G. I. (1993) *J. Biol. Chem.* 268, 14033-14039

8. Sato, H., Takino, T., Okada, Y., Cao, J., Shinagawa, A., Yamamoto, E., and Seiki, M. (1994) *Nature* 370, 61-65

9. Cao, J., Sato, H., Takino, T., and Seiki, M. (1995) *J. Biol. Chem.* 270, 801-805

10. Atkinson, S. J., Crabbe, T., Cowell, S., Ward, R. V., Butler, M. J., Sato, H..Seiki, M., Reynolds, J. J., and Murphy, G. (1995) *J. Biol. Chem.* 270, 30479-30485

11. Sato, H., Takino, T., Kinoshita, T., Imai, K., Okada, Y., Stetler-Stevenson. W. G., and Seiki, M. (1996) *FEBS Lett.* 385, 238-240

12. Sato, H., and Seiki, M. (1996) *J. Biochem. (Tokyo)* 119, 209-215

13. Pei, D., and Weiss, S. J. (1996) *J. Biol. Chem.* 271, 9135-9140

14. Maquoi, E., Noël, A., Frankenne, F., Angliker, H., Murphy, G., and Foidart. J.-M. (1998) *FEBS Lett.* 424, 262-266

15. Strongin, A. Y., Collier, I., Bannikov, G., Marnier, B. L., Grant, G. A., and Goldberg, G. I. (1995) *J. Biol. Chem.* 270, 5331-5338

16. Butler, G. S., Butler, M. J., Atkinson, S. J., Will, H., Tamura, T., Schade van Westrum, S., Crabbe, T., Clements, J., d'Ortho, M.-P., and Murphy, G. (1998) *J. Biol. Chem.* 273, 871-880

17. Cowell, S., Knäuper, V., Stewart, M. L., d'Ortho, M.-P., Stanton, H., Hembry, R. M., Lopez-Otin, C, Reynolds, J. J., and Murphy, G. (1998) *Biochem. J.* 331, 453-458

18. Kinoshita, T., Sato, H., Okada, A., Ohuchi, E., Imai, K, Okada, Y., and Seiki. M. (1998) *J. Biol. Chem.* 273, 16098-16103

19. Zucker, S., Drews, M., Conner, C, Foda, H. D., DeClerck, Y. A., Langley, K. E.. Bahou, W. F., Docherty, A. J. P., and Cao, J. (1998) *J. Biol. Chem.* 273, 1216-1222

20. Baramova, E, N, Bajou, K, Remade, A, L'Hoir, C, Krell, H. W., Weidle, U. H., Noël, A., and Foidart, J.-M. (1997) *FEBS Lett.* 405, 157-162

21. Sato, H., Kinoshita, T., Takino, T., Nakayama, K, and Seiki, M. (1996) *FEBS Lett.* 393, 101-104

22. Will, H., Atkinson, S. J., Butler, G. S., Smith, B., and Murphy, G. (1996) *J. Biol. Chem.* 271, 17119-17123

23. Ray, J. M., and Stetler-Stevenson, W. G. (1995) *EMBO J.* 14, 908-917

24. Hayakawa, T., Yamashita, K, Ohuchi, E., and Shinagawa, A. (1994) *J. Cell Sci.* 107, 2373-2379

25. Valente, P., Fassina, G., Melchiori, A., Masiello, L., Cilli, M., Vacca, A., Onisto, M., Santi, L., Stetler-Stevenson, W. G., and Albini, A. (1998) *Int. J. Cancer* 75,246-253

26. Farina, A, Tacconelli, A., Teti, A., Gulino, A., and Mackay, A. R. (1998) *Cancer Res.* 58, 2957-2960

27. Liotta, L. A. Steeg, P. S., and Stetler-Stevenson, W. G. (1991) *Cell* 64, 327-336

28. DeClerck, Y. A, Perez, N, Shimada, H., Boone, T. C, Langley, K. E., and Taylor, S. M. (1992) *Cancer Res.* 52, 701-708

29. Imren, S., Kohn, D. B., Shimada, H., Blavier, L., and DeClerck, Y. A. (1996) *Cancer Res.* 56, 2891-2895

30. Montgomery, A. M., Mueller, B. M., Reisfeld, R. A., Taylor, S. M., and DeClerck, Y. A. (1994) *Cancer Res.* 54, 5467-5473

31. Moses, M. A, Sudhalter, J., and Langer, R. (1990) *Science* 248, 1408-1410

32. Stetler-Stevenson, W. G., Krutzsch, H. C, and Liotta, L. A. (1989) *J. Biol. Chem.* 264, 17374-17378

33. Grigioni, W. F., D'Errico, A., Fortunato, C, Fiorentino, M., Mancini, A. M., Stetler-Stevenson, W. G., Sobel, M. E., Liotta, L. A, Onisto, M., and Garbisa, S. (1994) *Mod. Pathol.* 7, 220-225

34. Onisto, M., Riccio, M. P., Scannapieco, P., Caenazzo, C, Griggio, L., Spina, M., Stetler-Stevenson, W. G., and Garbisa, S. (1995) *Int. J. Cancer* 63, 621-626

35. Gohji, K-, Fujimoto, N., Fujii, A., Komiyama, T., Okawa, J., and Nakajima, M. (1996) *Cancer Res.* 56, 3196-3198

36. Campion, C, Dickens, J. P., and Crimmin, M. J. (May 31, 1990) PCT Patent WO 90/05719

37. Castelhano, A. L., Home, S., Shengyan, L., Castelhano, L. A., Krantz, A., Liak. J. T., Yuang, Z., and Liak, T. J. (February 16, 1995) PCT Patent WO 95/04735

38. Brown, P. D., Bawden, L., and Miller, K. (November 11, 1993) Patent WO 93/21942

39. Jensenius, J. C, Andersen, I., Hau, J., Crone, M., and Koch, C. (1981) *J. Immunol. Methods* 46, 63-68

40. Emmert-Buck, M. R., Emonard, H., Corcoran, M. L., Krutzsch, H. C, Foidart, J.-M., and Stetler-Stevenson, W. G. (1995) *FEBS Lett.* 364, 28-32

41. Cao, J., Rehemtulla, A., Bahou, W., and Zucker, S. (1996) *J. Biol. Chem.* 271, 30174-30180

42. Lehti, K, Lohi, J., Valtanen, H, and Keski-Oja, J. (1998) *Biochem. J.* 334, 345-353

43. Haigler, H. T., Maxfield, F. R., Willingham, M. C, and Pastan, I. (1980) *J. Biol. Chem.* 255, 1239-1241

44. Nakahara, H, Howard, L., Thompson, E. W., Sato, H., Seiki, M., Yeh, Y., and Chen, W.-T. (1997) *Proc. Natl. Acad. Sci. U. S. A.* 94, 7959-7964

45. Ng, G. Y., Trogadis, J., Stevens, J., Bouvier, M., O'Dowd, B. F., and George. S. R. (1995) *Proc. Natl. Acad. Sci. U. S. A.* 92, 10157-10161

46. Thekkumkara, T. J., Du, J., Dostal, D. E., Motel, T. J., Thomas, W. G., and Baker, K. M. (1995) *Mol. Cell. Biochem.* 146, 79-89

47. Bowman, E. J., Siebers, A, and Altendorf, K. (1988) *Proc. Natl. Acad. Sci. U. S. A.* 85, 7972-7976

48. Shofuda, K.-L, Moriyama, K, Nishihashi, A., Higashi, S., Mizushima, H, Yasumitsu, H, Miki, K, Sato, H, Seiki, M., and Miyazaki, K. (1998) *J. Biochem. (Tokyo)* 124, 462-470

49. d'Ortho, M.-P., Stanton, H, Butler, M., Atkinson, S., and Murphy, G. (1998) *FEBS Lett.* 421, 159-164

50. Lohi, J., Lehti, K, Westermarck, J., Kähäri, V.-M., and Keski-Oja, J. (1996) *Eur. J. Biochem.* 239, 239-247

51. Ellerbroek, S. M., Fishman, D. A, Kearns, A., Bafetti, L. M., and Stack, M. S. (1999) *Cancer Res.* 59, 1635-1641

52. Foda, H. D., George, S., Conner, C, Drews, M., Tompkins, D. C, and Zucker. S. (1996) *Lab. Invest.* 74, 538-545

53. Schwartz, A. L. (1995) *Pediatr. Res.* 38, 835-843

54. Clague, M. J., Urbe, S., Aniento, F., and Gruenberg, J. (1994) *J. Biol. Chem.* 269, 21-24

55. Oda, K-, Nishimura, Y., Ikehara, Y., and Kato, K. (1991) *Biochem. Biophys. Res. Commun.* 178, 369-377

56. Nykjær, A., Conese, M., Christensen, E. I., Olson, D., Cremona, O., Gliemann. J., and Blasi, F. (1997) *EMBO J.* 16, 2610-2620

57. Liotta, L. A, Stetler-Stevenson, W. G., and Steeg, P. S. (1991) *Cancer Invest.* 9, 543-551

58. Brown, P. D., and Giavazzi, R. (1995) *Ann. Oncol.* 6, 967-974

59. Wojtowicz-Praga, S. M., Dickson, R. B., and Hawkins, M. J. *(1997) Invest. New Drugs* 15, 61-75